ELSEVIER

Biophysical Chemistry 97 (2002) 203–212

Biophysical Chemistry

www.elsevier.com/locate/bpc

Fluorescence and nucleic acid binding properties of bovine leukemia virus nucleocapsid protein

David R. Morcock[a,*,1], Sudhakar Katakam[a,b,1], Bradley P. Kane[a,1], José R. Casas-Finet[a,c,1]

[a]*AIDS Vaccine Program, SAIC Frederick, National Cancer Institute at Frederick, Building 535, 5th floor, P.O. Box B, Frederick, Maryland 21702, USA*

[b]*Informax, Inc., 7600 Wisconsin Avenue, Suite #1100 Bethesda, MD 20814, USA*

[c]*MedImmune, Inc., 35 West Watkins Mill Road, Gaithersburg, MD 20878, USA*

Received 19 December 2001; received in revised form 8 March 2002; accepted 15 March 2002

Abstract

We used the intrinsic fluorescence of bovine leukemia virus p12, a nucleocapsid protein with two tryptophan-containing zinc fingers (ZFs), to study its conformation and binding to single-stranded nucleic acids. Spectral emission maxima suggested solvent-exposed tryptophans. A peptide derived from ZF1 had a higher quantum yield and longer average lifetime (τ) than ZF2. BLV p12 τ and rotational correlation time were greater than ZF values, but all demetallated sequences gave similar results. Apo p12 showed reduced fluorescence intensity, τ and loss of secondary structure. DNA-binding affinity of p12 was in the nanomolar range, and decreased 14-fold after Zn^{++} ejection. Nucleobase preference of BLV p12 was different from the closely related HTLV-1 but similar to HIV-1 and SIV nucleocapsids, both phylogenetically distant.

Keywords: Bovine leukemia virus; Nucleocapsid; Zinc finger; Fluorescence

1. Introduction

Retroviral nucleocapsid (NC) proteins are nucleic acid-binding proteins that package RNA inside the viral capsid, facilitate nucleic acid strand annealing and perform auxiliary functions in the viral replication cycle [1–3].

BLV p12, the nucleocapsid protein from bovine leukemia virus, has two tryptophan-containing zinc fingers (ZFs). Intrinsic fluorescence from tryptophan was used to study p12 conformation and its binding to single-stranded nucleic acids. Frequency-domain fluorescence and circular dichroism spectroscopy were used to assess the divalent ion binding by p12 protein and zinc finger peptides, as well as changes in the microenvironment of their tyrosine and tryptophan residues.

Based on our results, we compared p12 to NC proteins from other retroviruses: human and simian immunodeficiency viruses (HIV-1 and SIV), and human T-cell leukemia virus-type one (HTLV-1). Earlier studies have shown that HIV-1 and SIV

*Corresponding author. Tel.: +1-301-846-1644; fax: +1-301-846-5588.

E-mail address: morcock@ncifcrf.gov (D.R. Morcock).

[1] These authors contributed equally to this work.

0301-4622/02/$ - see front matter
PII: S0301-4622(02)00070-4

have similar nucleic acid binding properties [4,5], but the NC from HTLV-1 has radically different properties [6]. Since BLV is phylogenetically closely related to HTLV-1, we have obtained the nucleic acid binding properties of p12 and compared them to those of other retroviral NC proteins. Our findings demonstrate dissimilar binding affinity and base preference between HTLV-1 p15 and BLV p12, likely reflecting sub-family specific functional differences. Surprisingly, BLV p12 nucleic acid binding characteristics resembled HIV-1 p7 and SIV p8 more than HTLV-1 p15. The difference may be related to their isoelectric point (p*I*). HTLV-1 NC has a neutral p*I* (7.2), but BLV, SIV and HIV-1 NC all have p*I* values greater than 9.

2. Materials and methods

Nucleocapsid protein, p12, was isolated from BLV-infected fetal lamb kidney cells. A 10-ml sample of 10 mg/ml cell suspension was made 8 M in guanidine–HCl, 40 mM in Tris–hydrochloride, pH 8.5, and 2% (v/v) in 2-mercaptoethanol. After the suspension was mixed and allowed to sit at room temperature for 1 h, it was purified using reversed-phase HPLC as previously described [7]. Fractions containing p12 were identified by sodium dodecyl sulfate polyacrylamide gel electrophoresis and Coomasie Brilliant Blue staining, lyophilized, and rechromatographed. Viral protein was quantified by amino acid analysis; both the amino acid composition and molecular mass of the pooled p12 material were in agreement with that expected from the published sequence [8]. Zinc chloride was added to the purified p12 at 2 g atom per mole. Purified p12 was stored at −80 °C until used.

The amino acid sequence of BLV p12 is VHTPG[5] PKMPG[10] PRQPA[15] PKRPP[20] PGP**CY**[25] **RCLKE**[30] **GHWAR**[35] **DC**PTK[40] ATGPP[45] PGP**CP**[50] **ICKDP**[55] **SHWKR**[60] **DC**PTL[65] KSKN[69] [8]. The first and second zinc finger motifs, ZF1 and ZF2, are emphasized as bold, underlined sequences in the text. Peptides corresponding to residues 22–64 (containing each ZF domain and the linking residues), residues 22–39 (containing the ZF1 domain) and residues 47–64 (containing the ZF2 domain) were synthesized by Macromolecular Resources (Ft. Collins, CO). All peptides were characterized by HPLC and MALDI-TOF mass spectrometry. Sodium phosphate buffer (1 mM, pH 7.0) was used for all protein and peptide solutions. De-metallated protein and peptide was prepared by reaction with *N*-ethylmaleimide, added to five-fold excess of the cysteine content.

Circular dichroism spectra were collected with a Jasco J-720 spectropolarimeter from 260 to 190 nm with a 1-nm bandwidth, a data density of 10 points/nm, a scan rate of 10 nm/min, and a time constant of 16 s. Samples were placed in demountable (both ends closed) quartz Suprasil cuvettes (Uvonic Instruments, Plainview, NY) with a path length of 0.5 mm. Samples (1 mg/ml) were dissolved in 1 mM sodium phosphate, pH 7.0.

Dynamic fluorescence lifetime and anisotropy measurements were made with a 10-GHz frequency-domain fluorometer using the frequency-doubled output (296 nm) of a Rhodamine-6G tunable dye laser as described by Laczko et al. [9]. Analysis of fluorescence emission phase angle and modulation when excitation light intensity is modulated with increasing frequency yields lifetime and pre-exponential coefficients of individual components in the fluorescence decay profile. Equations for fitting the dynamic frequency data have been reported previously [10].

Steady state fluorescence was measured in a Shimadzu RF-5301PC spectrofluorometer. Spectra of p12 and zinc finger peptides were collected, using excitation at 280 and 295 nm to distinguish tryptophan and tyrosine contributions. Excitation bandwidth was 1.5 nm; emission bandwidth was 5 nm. Spectra of de-metallated p12 and peptides were collected immediately after adding excess Na_4 EDTA.

Fluorometric titrations of BLV p12 and related peptides with single-stranded nucleic acid were carried out in 1 mM sodium phosphate, pH 7.0, using the method of Kelly et al. [11]. Solutions were kept at 25 °C in dual-pathlength (2×10 mm) capped Suprasil quartz cells (Uvonic Instruments); emission was recorded at 350 nm. Oligonucleotides were quantified by UV absorbance.

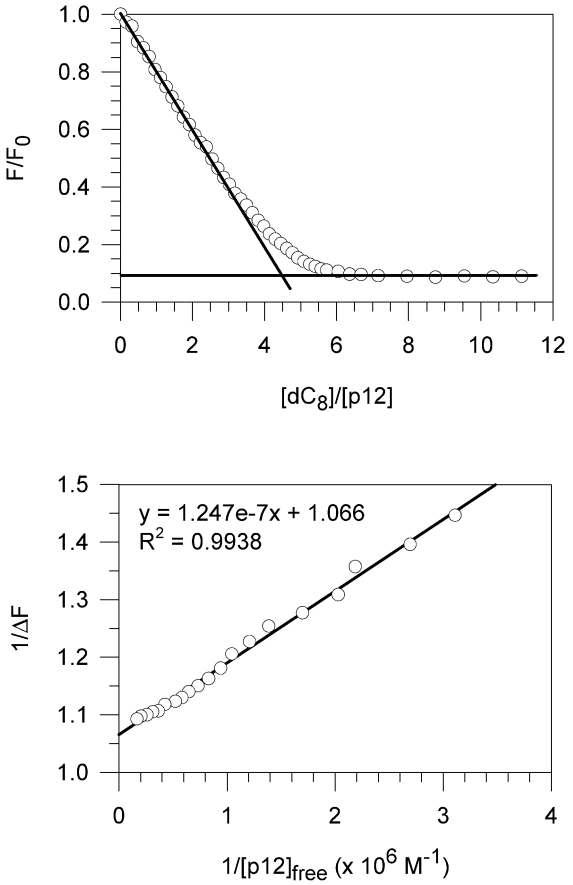

Fig. 1. (Upper) Normalized fluorescence vs. concentration ratio of nucleic acid to protein. $(dC)_8$ was added to p12 (1 μM in 1 mM sodium phosphate, pH 7.0). The plateau's intersection with the initial slope indicates the stoichiometry (n, occluded binding site size in the case of a polynucleotide) for a titration carried out under near-stoichiometric conditions such as that shown. (Lower) Double-reciprocal plot. The y-intercept is the reciprocal of the fluorescence fraction quenched; binding affinity is n/m, where m is the slope of the regression line.

Occluded binding site size, limiting quenching, and binding affinity were calculated from graphs of relative fluorescence intensity vs. [nucleic acid base]/[protein] ratio after correction for dilution and the inner filter effect (Fig. 1). The analysis binding constants in Table 2 are macroscopic. In the case of polynucleotides, cooperativity was analyzed on a Scatchard plot using the model of McGhee and von Hippel. For oligonucleotides, a single site binding mode was assumed for all homopolymeric lattices used. The number of ionic interactions and the non-electrostatic contribution to the free energy of binding were derived from salt back-titrations in which 5 M NaCl was incrementally added to disrupt the protein-nucleic acid complex, resulting in fluorescence recovery (Fig. 2) [12]. Binding cooperativity was calculated using the model developed by McGhee and von Hippel [13].

Low salt buffer was used in the initial titrations to maximize nucleic acid binding to p12 and to

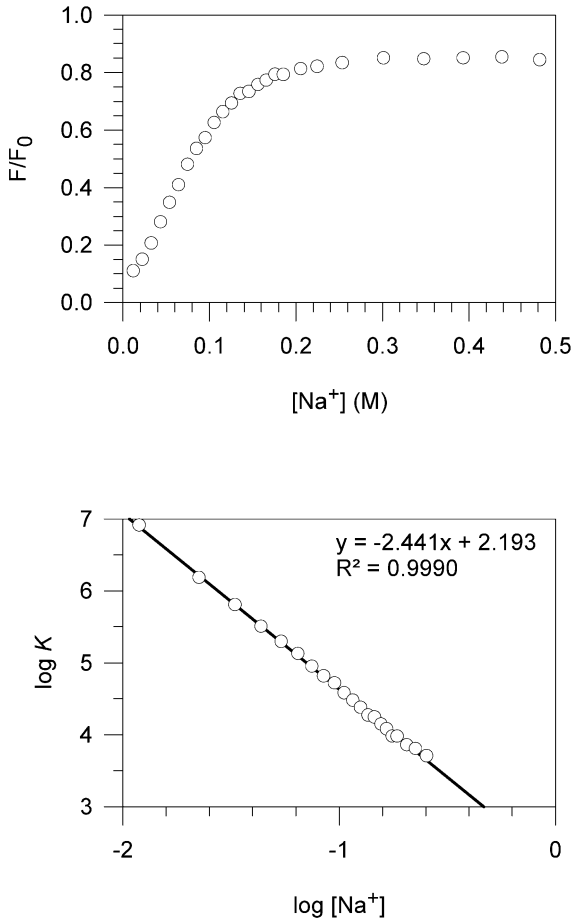

Fig. 2. (Upper) Fluorescence recovery after the addition of 5 M NaCl aliquots to a pre-formed p12-$d(C)_8$ complex. (Lower) Double-logarithmic plot. The slope divided by 0.71 indicates the number of Na^+ ions displaced; the y-intercept is log $K°$ at 1 M [Na^+], when only non-ionic interactions contribute to binding free energy.

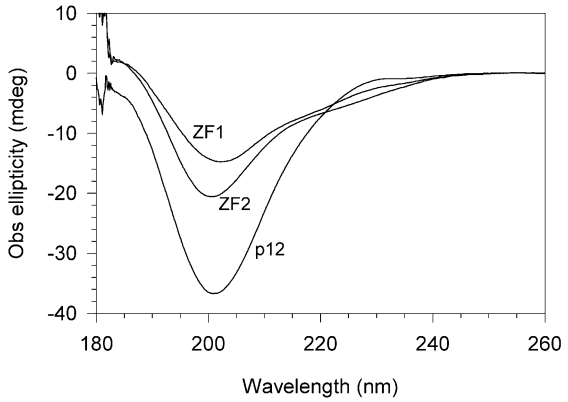

Fig. 3. CD spectra of BLV p12, ZF1 and ZF2. Solutions were 1 mg/ml in 1 mM sodium phosphate, pH 7.0.

allow a broader range of salt concentrations to be explored in the subsequent salt-back titration. Linearity of the log K vs. log $[Na^+]$ plots verified that no change in the thermodynamic binding mode of BLV NC occurred over the $[Na^+]$ range used in this study.

3. Results

3.1. Circular dichroism spectroscopy

Circular dichroism spectroscopy of BLV NC and ZF sequences yielded spectra (Fig. 3) nearly identical to those reported earlier for a number of NC proteins and peptides of retroviral origin [14–18]. CD spectra showed similar folding for Zn^{++}-bound p12, ZF1 and ZF2, characteristic in all cases of a tightly folded α/β structure. Apo-p12 peptides showed a 2–3 nm blue shift at the spectral extrema and slight band narrowing, as well as increased intensity of a negative ellipticity band at 200 nm (not shown), indicating loss of secondary structure and an increase in aperiodic component. These results are similar to those observed for a 39-residue peptide containing the two zinc-binding domains of the HIV-1 nucleocapsid protein [17] and confirm that all BLV p12 sequences were bound to Zn^{++} under our experimental conditions.

3.2. Steady state fluorescence spectroscopy

BLV p12 emission peaked at 348 nm, indicating partial tryptophan exposure to solvent (Fig. 4). The sole tyrosine in p12, found within ZF1, accounted for 2% of p12 and 9% of ZF1 overall emission, suggesting very efficient energy transfer to both Trp33 in ZF1 and Trp58 in the second finger. Consequently, close proximity of the ZF domains in the full-length protein was inferred.

De-metallated p12 emission λ_{max} was 352 nm; intensity was only 23% of native p12 intensity (Fig. 4), but the tyrosine contribution increased to 6% of total emission intensity. These observations reflect the unfolding of the ZF domains, allowing more frequent deactivation of tryptophan's excited state (possibly by collisions with the other residues), and an increase in the Tyr–Trp distance that decreases the extent of single-singlet energy transfer.

ZF1 and ZF2 emission were strongest at 353 nm, suggesting that tryptophan is more solvent-exposed in the ZF peptides than in p12; a synthetic double ZF peptide had maximum emission at 350 nm, between the p12 and ZF peptide maxima. This is consistent with inter-ZF domain proximity, which would be responsible for mutual solvent shielding in p12.

3.3. Frequency-domain fluorescence spectroscopy

To further characterize the microenvironment of the aromatic side chains in the p12 ZF domains,

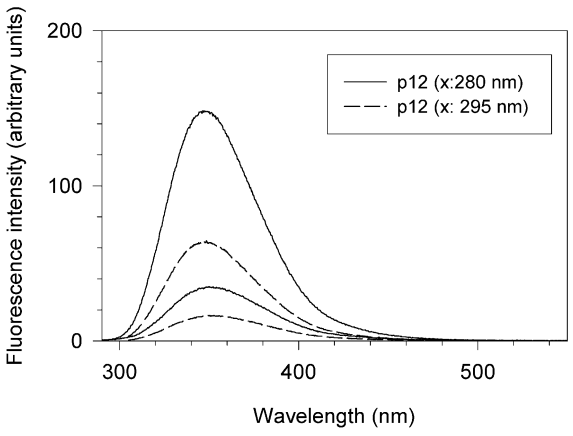

Fig. 4. BLV p12 (10 μg/ml in 1 mM sodium phosphate, pH 7.0) emission using excitation at 280 (solid lines) and 295 nm (dashed lines). Spectra were recorded before and after adding excess EDTA. The lower line in each pair represents intensity after EDTA addition.

Table 1
BLV-1 p12 fluorescence lifetime data

System	τ_1/ns	τ_2/ns	τ_1	τ_2	SS1	SS2	τ_{avg}/ns	χ^2
p12	0.47±0.03	4.77±0.11	0.82	0.17	0.28	0.60	3.40	1.1
apo p12	0.46±0.02	2.19±0.04	0.61	0.39	0.25	0.75	1.76	1.0
ZF1	0.92±0.04	5.02±0.10	0.61	0.39	0.22	0.78	4.11	1.1
apo ZF1	0.45±0.04	2.18±0.06	0.63	0.37	0.26	0.74	1.75	1.1
ZF2	0.69±0.03	3.37±0.07	0.57	0.43	0.21	0.79	1.84	1.0
apo ZF2[a]	0.04±0.02	2.05±0.05	0.95	0.05	0.24	0.70	1.54	1.6

[a] A long-lived emission background of approximately 130 ns, accounting for 6% of the steady state intensity was factored in the deconvolution of the dynamic fluorescence response.

τ: tryptophan fluorescence decay lifetime; α normalized pre-exponential coefficient; SS: steady state intensity of fluorescence component; τ_{avg}: average fluorescence lifetime.

dynamic fluorescence experiments were carried out. The average fluorescence lifetime (τ_{avg}) of ZF1 exceeds that of ZF2 (Table 1), suggesting dissimilar indole ring dynamics in the two ZFs. The τ_{avg} of full-length p12 is an average of the τ_{avg} values of its constituent zinc fingers. A comparison of the pre-exponential coefficients and lifetimes of the individual components in p12, ZF1 and ZF2 suggests complex tryptophan dynamics or energy migration between Trp^{33} and Trp^{58}. In the absence of Zn^{++}, the lifetime values and fractional contributions to the steady state intensities of full-length p12, ZF1 and ZF2 became indistinguishable, suggesting that any differences in these properties between the various sequences arise mostly from changes in Trp microenvironment in the folded state. It is worth noting the dominant pre-exponential component of a very short ($\sim$40 ps) lifetime in the decay of apoZF2 (Table 1). We attribute this short component to the presence of a neighboring lysine residue adjacent to Trp^{58} in the second zinc finger motif. The increased mobility of both the indole side chain of Trp and the ε-amino group of Lys upon loss of Zn(II) chelation are likely to facilitate the annihilation of the Trp excited singlet state by either collisional deactivation or charge transfer.

The average lifetime of p12 was reduced by half after Zn^{++} displacement (Table 1), in agreement with steady-state results. Since the reduction in fluorescence emission intensity was less pronounced (30%) than the decrease in τ_{avg} (50%) upon Zn^{++} displacement, and the loss in Tyr–Trp energy transfer cannot fully account for the difference, we infer an increase in the Trp quantum yield of apo-p12, relative to its Zn^{++}-bound state. This could result from partial occlusion of the indole rings among themselves or with Tyr^{25}, the only other aromatic residue in the p12 primary sequence, in a close proximity conformation present only in the native state.

In agreement with this hypothesis, the rotational correlation time of p12 (ϕ, 1.4 ns) exceeds ZF1 ϕ and ZF2 ϕ (0.81 ns for both), as expected if the two ZFs were not able to move independently but showed instead a degree of correlated (rigid body) motion. Apo-p12 ϕ (0.69 ns) decreased to a value similar to apo ZF1 ϕ (0.49 ns) and ZF2 ϕ (0.57 ns). Our results, taken together, suggest strongly that ZF-ZF interactions are responsible for the reduction in p12 ϕ and indicate that the inter-ZF proximity requires folded, native domains for its occurrence.

3.4. Polynucleotide binding

BLV p12 bound to polynucleotides with no preference detected between DNA and RNA (Table 2). Occluded binding site size was 4±2. Cooperativity of p12-polynucleotide binding was marginal, as seen for HIV-1 and SIV NCs [4,19]. Reaction with *N*-ethylmaleimide (NEM), which alkylates cysteine residues, results in divalent metal ejection and unfolding of the zinc finger domains, generating apo p12; this reduced polynucleotide binding affinity 14-fold (Table 2).

Katoh et al. reported a 3–4 increase in apo-p12 binding to RNA when in the presence of Zn^{++}, as measured by a gel retardation assay [20]. This is in line with our results, although the magnitude of binding affinity lost through zinc ejection is lower.

The extent of functional impairment seen after NEM-reaction was less than that observed for SIV NC [4], reflecting the relatively low affinity of p12 in its native state for nucleic acid. Conversely, HIV-1 NC had increased affinity for polyethenoadenylic acid after NEM-reaction, although the affinity of native HIV-1 NC in the presence of EDTA and dithiothreitol decreased 20-fold [19]. Apo-p12 bound polynucleotides with a significant decrease in its occluded binding site size, limiting quenching at saturation, and relative contribution of the electrostatic and non-electrostatic components of the binding free energy, suggesting a radically different interaction with the nucleic acid lattice.

Titrations carried out with zinc finger peptides were characterized by 2–3 orders of magnitude lower affinity and much lower limiting fluorescence quenching, showing decreased involvement of Trp-containing binding centers in these sequences. No shift of fluorescence emission maximum wavelength was observed as expected from complete quenching of Trp side chains in a stacked conformation with nucleic acid bases [21].

Additional evidence for the pivotal role of tryptophan residues in the nucleic acid binding reaction was gathered from the observed correlation between the limiting quenching of indole fluorescence and the observed binding energy (Fig. 5). Deoxythymidine and uridine give 80–82% quenching with BLV p12 as 8-mer oligos, 88–89% as polynucleotides (Table 2). However, the full-length apo-p12 shows 54% quenching with poly(dT) (Table 2); the double zinc finger shows 37% quenching with poly(dT), and zinc finger 2 shows 17% quenching with poly(U) (Fig. 5). Such correlation probably stems from the fact that tryp-

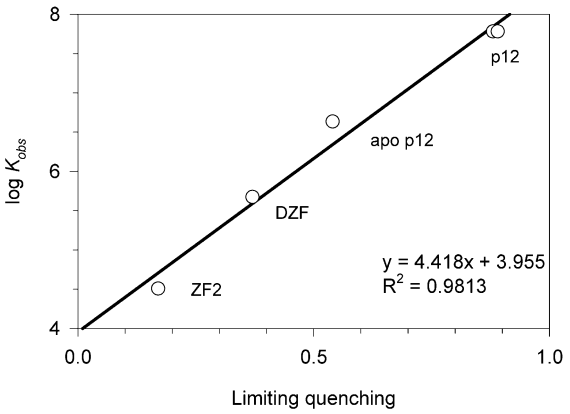

Fig. 5. Limiting quenching vs. log K_{obs} of p12 bound to either poly (U) or poly (dT). Binding affinity of p12 at 1 M NaCl correlates well with Trp emission quenching, indicative of less intimate interaction with nucleic acid as the protein is truncated.

Table 2
Nucleic acid binding properties of BLV p12 in 1 mM NaP, pH 7.0

Ligand	% Quenching	K_{obs} ($\times 10^7$ M^{-1})	Slope	log $K°$
poly (dT)	88	6±4	−3.4	1.5
poly (U)	89	6±1	−3.1	1.3
$(dG)_8$	76	14±4	−2.6	2.6
$(dI)_8$	76	6±1	−2.2	2.1
$(dC)_8$	92	5.0±0.7	−2.5	2.2
$(dT)_8$	82	2±1	−2.1	1.5
$(dU)_7dT$	80	1.2±0.6	−2.2	1.1
$(dA)_8$	56	0.12±0.01	−1.6	1.4
apo p12 + poly (dT)	54	0.43±0.09	−2.0	3.3

K_{obs}: observed binding affinity. Slope: slope of the double-logarithmic plot derived from salt-back titration. log $K°$: y-intercept of the double-logarithmic plot.

tophan side chains dominate the overall fluorescence emission of BLV p12, and constitute the largest component of the non-electrostatic contribution to the standard Gibbs free energy. Consequently, less intimate interaction between the indole ring of Trp and the thymine (or uracil) base would reduce both fluorescence quenching and binding affinity.

3.5. Oligonucleotide binding

BLV p12 showed a marked reduction in tryptophan fluorescence emission intensity upon addition of increasing amounts of short oligonucleotides (Fig. 1 upper panel). Maximum fluorescence quenching varied from 56 to 92% (Table 2). Notwithstanding the fact that purines (with a fused six-membered and a five-membered nitrogen-containing ring) could be expected to induce a larger overlap with the indole ring of tryptophan than pyrimidines (with only a six-membered ring), pyrimidines induced greater quenching than purines (Table 2), perhaps reflecting a more closely intercalated nucleobase-aromatic side chain structure. Binding affinity was derived from double reciprocal plots (Fig. 1 lower panel) as described [11]. BLV p12 binding affinity varied with oligonucleotide bases. The base preference in octanucleotide binding was $G > I \approx C > T \approx U > A$; binding affinity spanned two orders of magnitude (Table 2). This range was more compressed than for all other retroviral NCs examined, except HTLV-1 p15. The average occluded binding site size for all oligonucleotides was 5.0, comparable to that observed for polynucleotide lattices.

3.6. Ionic interactions

Back titrations with NaCl result in the recovery of p12 fluorescence (Fig. 2, upper panel), and suggest a net displacement of 3–4 ions in the p12-nucleic acid complex (Fig. 2, lower panel and Table 2). Identical number of displaced counterions were seen in HIV-1 and SIV, but not HTLV-1 NCs, confirming the closer functional relationship of BLV p12 to the former sequences. Anion uptake or release was not investigated in this study. Protonation and hydration effects on the double-logarithmic trace are considered unlikely since the system is buffered to constant pH and the maximum [NaCl] required to fully dissociate the BLV p12-nucleic acid complex is under 0.3 M (see Fig. 2) where the effect on water activity is minimal. Oligonucleotide binding exhibited a slope in the double-logarithmic plots derived from salt-back titrations with an average value of 2.2 ± 0.3, compared to that of 3.3 ± 0.2 seen for polynucleotides (Table 2). This suggests that binding to single-site sequences induces a reduction in the number of counterions displaced upon complex formation, and accounts for the $\sim$4-fold tighter binding of BLV p12 to longer lattices of uniform base composition (compare the affinity for T or U poly- vs. oligonucleotide sequences in Table 2).

4. Discussion

4.1. Spectroscopy

Circular dichroism, dynamic and steady state fluorescence spectroscopy indicated that all BLV ZF sequences bound Zn^{++} and folded similarly. Tryptophan's solvent exposure was considerable in p12 and increased after Zn^{++} removal. Close proximity between the two ZF domains was suggested by higher tryptophan exposure in ZF1 and ZF2 peptides, relative to p12, as well as higher quantum yield and longer average fluorescence lifetime and dynamic anisotropy in the Zn^{++}-bound protein and ZF peptides, but not in the demetallated systems. The presence of two highly similar ZF domains in p12, each possessing a hydrophobic, planar Trp side chain (as in the case of SIV p8) suggests that both ZFs are involved in its association with nucleic acids.

4.2. Nucleic acid binding

Nucleic acid binding affinity of BLV p12 falls between reported values for HIV-1/SIV and HTLV-1 (Fig. 6). Interestingly, the nucleic acid base preference and binding affinity of BLV p12 resembles HIV-1 and SIV preferences more than the phylogenetically closer HTLV-1. Ranked by binding affinity, nucleobase preferences (excepting cytosine) are identical for BLV p12, HIV-1 p7,

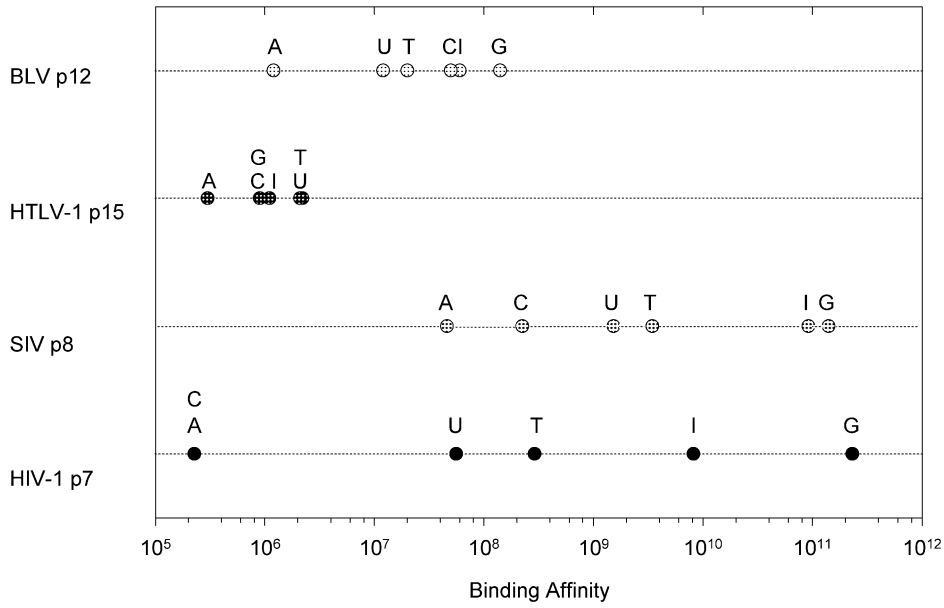

Fig. 6. Graphical comparison of the binding affinity at 1 mM sodium phosphate, pH 7.0, of NC proteins from BLV, HTLV-1 [6], SIV [4], and HIV-1 [5] for homopolymeric deoxynucleotides. Values exceeding $\sim 10^8$ M^{-1} are extrapolated to low-salt conditions from the known salt dependence of binding affinity.

and SIV p8 (Fig. 6); HTLV-1 p15 has a considerably different order of base preference. Adenine binds worst in each case, perhaps due to the strong tendency of A bases to form stacked structures [22]. In all cases except HTLV-1 p15, G shows the highest binding affinity for Trp-containing retroviral NC proteins. G-rich sequences have been shown to occur in the encapsidation signals of several retroviruses, including HIV-1 [23,24], SIV [25], HTLV-1 [26], and murine leukemia virus genomes [27]. BLV packaging signal sequence [28,29], however, is not G-rich.

HIV-1 and SIV are closely related retroviruses, and their nucleocapsid proteins bind with similar base preferences [4,5]; binding affinities span several orders of magnitude (Fig. 6). HTLV-1 and BLV are another pair of closely related retroviruses. Thus, we expected their NC proteins would also have similar base preferences. However, our results show that the two proteins, BLV p12 and HTLV-1 p15, have different nucleic acid binding properties. Even though BLV and HTLV-1 are closely related, their nucleocapsid proteins apparently function differently. Base preference, binding affinity and site size are all dissimilar for these two proteins. BLV p12 binding affinity spans two orders of magnitude, but HTLV-1 p15 affinity barely spans one. The comparatively narrow range and low average value of nucleic acid affinity for the leukemia retroviruses may contribute to the low infectivity observed for this retroviral subfamily.

Further research to characterize nucleic acid binding by other retroviral nucleocapsid proteins would establish whether NCs generally have similar nucleic acid binding properties (base preferences in this instance), as is the case with HIV-1, SIV, and BLV, or retroviral NCs have a range of preferences. A comparative study is currently underway in our laboratory. If diverse NC proteins do bind differently, it would lead to the conclusion that similarity of reverse transcriptase sequence, the basis for retroviral phylogeny, does not necessarily correlate with all aspects of biochemical function for retroviruses.

Acknowledgments

Part of this work was performed at the Center for Fluorescence Spectroscopy, University of Maryland at Baltimore School of Medicine. This research was done by SAIC Frederick under contract N01-CO-56000 from the National Cancer Institute. The content of this publication does not necessarily reflect the views or policies of the Department of Health and Human Services, nor does mention of trade names, commercial products, or organizations imply endorsement by the US Government.

References

[1] A. Rein, L.E. Henderson, J.G. Levin, Nucleic-acid-chaperone activity of retroviral nucleocapsid proteins: significance for viral replication, Trends Biochem. Sci. 23 (1998) 297–301.

[2] J.-L. Darlix, M. Lapadat-Tapolsky, H. de Rocquigny, B.P. Roques, First glimpses at structure-function relationships of the nucleocapsid protein of retroviruses, J. Mol. Biol. 254 (1995) 523–537.

[3] V.M. Vogt, in: J.M. Coffin, S.H. Hughes, H.E. Varmus (Eds.), Retroviruses, Cold Spring Harbor Laboratory Press, Plainview, NY, 1998, pp. 27–69.

[4] M.A. Urbaneja, C.F. McGrath, B.P. Kane, L.E. Henderson, J.R. Casas-Finet, Nucleic acid binding properties of simian immunodeficency virus nucleocapsid protein NCp8, J. Biol. Chem. 275 (2000) 10394–10404.

[5] J.Q. Wu, A. Ozarowski, A.H. Maki, M.A. Urbaneja, L.E. Henderson, J.R. Casas-Finet, Binding of the nucleocapsid protein of type 1 human immunodeficiency virus to nucleic acids studied using phosphorescence and optically detected magnetic resonance, Biochemistry 36 (1997) 12506–12518.

[6] D.R. Morcock, B.P. Kane, J.R. Casas-Finet, Fluorescence and nucleic acid binding properties of the human T-cell leukemia virus-type 1 nucleocapsid protein, Biochim. Biophys. Acta 1481 (2000) 381–394.

[7] L.E. Henderson, R.C. Sowder, G.W. Smythers, R.E. Benveniste, S. Oroszlan, Purification and N-terminal amino acid sequence comparisons of structural proteins from retrovirus-D/Washington and Mason–Pfizer monkey virus, J. Virol. 55 (1985) 778–787.

[8] T.D. Copeland, M.A. Morgan, S. Oroszlan, Complete amino acid sequence of the nucleic acid-binding protein of bovine leukemia virus, FEBS Lett. 156 (1983) 37–40.

[9] G. Laczko, I. Gryczynski, Z. Gryczynski, W. Wiczk, H. Malak, J. Lakowicz, A 10-GHz frequency-domain fluorometer, Rev. Sci. Instrum. 61 (1990) 2331–2337.

[10] J.R. Lakowicz, Principles of Fluorescence Spectroscopy, Plenum Press, NY, 1983.

[11] R.C. Kelly, D.E. Jensen, P.H. von Hippel, DNA 'melting' proteins. IV. Fluorescence measurements of binding parameters for bacteriophage T4 gene 32-protein to mono-, oligo-, and polynucleotides, J. Biol. Chem. 251 (1976) 7240–7250.

[12] M.T. Record, T.M. Lohman, P. de Haseth, Ion effects on ligand–nucleic acid interactions, J. Mol. Biol. 107 (1976) 145–158.

[13] J.D. McGhee, P.H. von Hippel, Theoretical aspects of DNA-protein interactions: co-operative and non-co-operative binding of large ligands to a one-dimensional homogeneous lattice, J. Mol. Biol. 86 (1974) 469–489.

[14] X. Chen, M. Chu, D.P. Giedroc, Spectroscopic characterization of Co(II)-, Ni(II)-, and Cd(II)- substituted wild-type and non-native retroviral-type zinc finger peptides, J. Biol. Inorg. Chem. 5 (2000) 93–101.

[15] L.M. Green, J.M. Berg, Retroviral nucleocapsid protein-metal ion interactions: folding and sequence variants, Proc. Natl. Acad. Sci. USA 87 (1990) 6403–6407.

[16] C.J. Gregoire, D. Gautheret, E.P. Loret, No tRNA3Lys unwinding in a complex with HIV NCp7, J. Biol. Chem. 272 (1997) 25143–25148.

[17] J.G. Omichinski, G.M. Clore, K. Sakaguchi, E. Appella, A.M. Gronenborn, Structural characterization of a 39-residue synthetic peptide containing the two zinc binding domains from the HIV-1 p7 nucleocapsid protein by CD and NMR spectroscopy, FEBS Lett. 292 (1991) 25–30.

[18] A. Surovoy, J. Dannull, K. Moelling, G. Jung, Conformational and nucleic acid binding studies on the synthetic nucleocapsid protein of HIV-1, J. Mol. Biol. 229 (1993) 94–104.

[19] M.A. Urbaneja, B.P. Kane, D.G. Johnson, R.J. Gorelick, L.E. Henderson, J.R. Casas-Finet, Binding properties of the human immunodeficiency virus type 1 nucleocapsid protein p7 to a model RNA: elucidation of the structural determinants for function, J. Mol. Biol. 287 (1999) 59–75.

[20] I. Katoh, H. Kyushiki, Y. Sakamoto, Y. Ikawa, Y. Yoshinaka, Bovine leukemia virus matrix-associated protein MA(p15): further processing and formation of a specific complex with the dimer of the 5′- terminal genomic RNA fragment, J. Virol. 65 (1991) 6845–6855.

[21] C. Hélène, J.C. Maurizot, Interactions of oligopeptides with nucleic acids, CRC Crit. Rev. Biochem. 10 (1981) 213–258.

[22] C.R. Cantor, P.R. Schimmel, Biophysical Chemistry Part I: The Conformation of Biological Macromolecules, W.H. Freeman and Co, New York, 1980.

[23] J. Clever, C. Sassetti, T.G. Parslow, RNA secondary structure and binding sites for gag gene products in the 5′ packaging signal of human immunodeficiency virus type 1, J. Virol. 69 (1995) 2101–2109.

[24] A. Zeffman, S. Hassard, G. Varani, A. Lever, The major HIV-1 packaging signal is an extended bulged stem loop whose structure is altered on interaction with the Gag polyprotein, J. Mol. Biol. 297 (2000) 877–893.

[25] T.A. Rizvi, A.T. Panganiban, Simian immunodeficiency virus RNA is efficiently encapsidated by human immunodeficiency virus type 1 particles, J. Virol. 67 (1993) 2681–2688.
[26] A.N. Jewell, L.M. Mansky, In the beginning: genome recognition, RNA encapsidation and the initiation of complex retrovirus assembly, J. Gen. Virol. 81 (2000) 1889–1899.
[27] M. Mougel, Y. Zhang, E. Barklis, cis-active structural motifs involved in specific encapsidation of Moloney murine leukemia virus RNA, J. Virol. 70 (1996) 5043–5050.
[28] L.M. Mansky, A.E. Krueger, H.M. Temin, The bovine leukemia virus encapsidation signal is discontinuous and extends into the 5′ end of the gag gene, J. Virol. 69 (1995) 3282–3289.
[29] L.M. Mansky, R.M. Wisniewski, The bovine leukemia virus encapsidation signal is composed of RNA secondary structures, J. Virol. 72 (1998) 3196–3204.